1 Summaries of Experimental Activities

1.1 E91-011

Investigation of the $N \to \Delta$ Transition via Polarization Observables in Hall A

S. Frullani, J.J. Kelly, and A.J. Sarty, Spokespersons,
and
the Hall A Collaboration.

Recoil polarization observables can provide new insight into properties of nucleon resonances and the reaction mechanisms for electroproduction of mesons by providing access to interference between small amplitudes and dominant amplitudes. The dominant amplitude for pion electroproduction at the Δ resonance is the M_{1+} multipole, but there is much current interest in the smaller S_{1+} amplitude that arises from configuration mixing within the quark core [1], often described as quadrupole deformation, or from meson and gluon exchange currents between quarks [2], or coupling to the pion cloud outside the quark core [3,4]. Observables which depend upon real parts of interference products are sensitive to these quadrupole amplitudes, but reliable interpretation of such data requires understanding background contributions from nonresonant production mechanisms and from underlying nondominant resonances. Sensitivity to background amplitudes is provided by observables which depend upon the imaginary parts of similar interference products. Experiment 91-011 was designed to measure both types of observables for the $p(\vec{e}, e'\vec{p})\pi^0$ reaction using the focal-plane polarimeter.

Our implementation of the R-function method for the cross section analysis was discussed in the progress report for 2001. Cross sections were extracted for a $5 \times 2 \times 20 \times 12$ grid in (W, Q^2, x_{cm}, ϕ) where W is the invariant mass of the πN system, Q^2 is the photon virtuality, $x_{cm} = \cos(\theta_\pi)$ is obtained from the pion angle in the cm, and ϕ is the azimuthal angle. Results for $W = 1.22 \pm 0.02$ GeV and $Q^2 = 0.9 \pm 0.1$ (GeV/c)^2 are compared in Fig. 1 with several recent models [5–7] and with a multipole analysis described below.

Polarization observables and the corresponding response functions were extracted using the maximum likelihood method. The likelihood function for the response function analysis takes the form

$$L = \prod_{i=1}^{N} \frac{1}{2\pi}(1 + \epsilon_x \sin\phi_{fpp} + \epsilon_y \cos\phi_{fpp}) \tag{1}$$

where

$$\epsilon_\alpha = \xi_\alpha + A(\theta_{fpp}) \sum_\beta S_{\alpha\beta}(P_\beta + hP'_\beta) \tag{2}$$

is the azimuthal asymmetry for a polarization $\vec{\Pi} = \vec{P} + h\vec{P}'$ with helicity-independent and helicity-dependent contributions, $\vec{P}$ and $\vec{P}'$, in the πN cm system at the target transformed to the focal-plane coordinate system by the spin-transport matrix

$S_{\alpha\beta}$. The FPP analyzing power and false asymmetry are $A(\theta_{fpp})$ and ξ_α. The polarizations are then expanded in response functions, R_η, according to

$$\sigma P_\beta = \sum_\eta \nu_{\beta\eta}(\epsilon, \phi) R_\eta \tag{3}$$

where σ is the differential cross section and where the kinematic coefficients, $\nu_{\beta\eta}$, depend upon the transverse polarization of the virtual photon, ϵ, and the azimuthal angle, ϕ. Thus, for a fixed model of the differential cross section the logarithm of the likelihood function is linear in the polarized response functions with coefficients that are accumulated event by event. The data were binned with respect to (W, Q^2, x_{cm}); the bins for (W, Q^2) match the cross section analysis but the nonuniform spacing in x_{cm} is designed to better utilize the lower statistics of the polarization data. Acceptance-averaged response functions were then obtained by maximizing the likelihood with respect to the response functions and their uncertainties were obtained from the covariance matrix.

Polarized response functions for a representative bin, $W = 1.22 \pm 0.02$ GeV and $Q^2 = 0.9 \pm 0.1$ (GeV/c)^2, are shown in Fig. 2 where the first set contributes in plane while the second set is obtained from the out-of-plane acceptance. The labeling distinguishes L, T, LT, and TT contributions to the unpolarized (0) cross section and to sideways (S), normal (N), or longitudinal (L) components of recoil polarization with an h to indicate helicity dependence, if any. Linear combinations that cannot be resolved without Rosenbluth separation are identified by L+T. These data are compared with the MAID2000, SAID, and DMT models. There is relatively little variation among models for those response functions that are dominated by multipole amplitudes for the Δ resonance but there are much larger variations for those, such as R_{LT}^N or R_{LT}^S, with significant background contributions from nonresonant mechanisms or nondominant (higher) resonances. The DMT model seems to provide the best overall fit to these data while the SAID model has the most difficulty with R_{LT}^N or R_{LT}^S, but none of these models provides a uniformly good fit to all response functions.

We have begun studying the sensitivity of the data to variations of the multipole amplitudes, but the results are still preliminary. The basic idea is to represent a multipole amplitude, $A_i(W, Q^2)$, in the form

$$A_i(W, Q^2) = A_i^{(0)}(W, Q^2) + \delta A_i(W, Q^2) \tag{4}$$

where $A^{(0)}$ is obtained from a suitable baseline model, here taken to be MAID2000, and δA is an adjustable parameter to be fitted to the data. The analysis fits all cross section and polarization response-function data that are available in a (W, Q^2) bin simultaneously. Adjustments to the magnetic, electric, and scalar amplitudes for a subset of the contributing partial waves are fit while maintaining the remaining amplitudes at their input (baseline) values. Examples of this procedure are shown in Fig. 3. The E_{0+} and S_{0+} amplitudes are highly correlated in the fit, so we somewhat arbitrarily chose to vary the real parts and not the imaginary parts; nor did we vary amplitudes for $\ell \geq 2$ at this stage. Although the wisdom of these selections will require further investigation, it is clear that the fit to data can be improved with relatively modest variations of the multipole amplitudes.

References

[1] N. Isgur, G. Karl, and R. Koniuk, Phys. Rev. **D 25**, 2394 (1982).

[2] A. J. Buchmann, arXiv:hep-ph/9909385 (unpublished).

[3] M. Fiolhais, G. Golli, and S. Sirca, Phys. Lett. **B373**, 229 (1996).

[4] S. S. Kamalov and S. N. Yang, Phys. Rev. Lett. **83**, 4494 (1999).

[5] D. Drechsel, O. Hanstein, S. S. Kamalov, L. Tiator, and S. N. Yang, www.kph.uni-mainz.de/MAID.

[6] R. A. Arndt, W. J. Briscoe, R. L. Workman, and I. I. Strakovsky, gwdac.phys.gwu.edu.

[7] S. S. Kamalov, S. N. Yang, D. Drechsel, O. Hanstein, and L. Tiator, Phys. Rev. **C 64**, 032201(R) (2001).

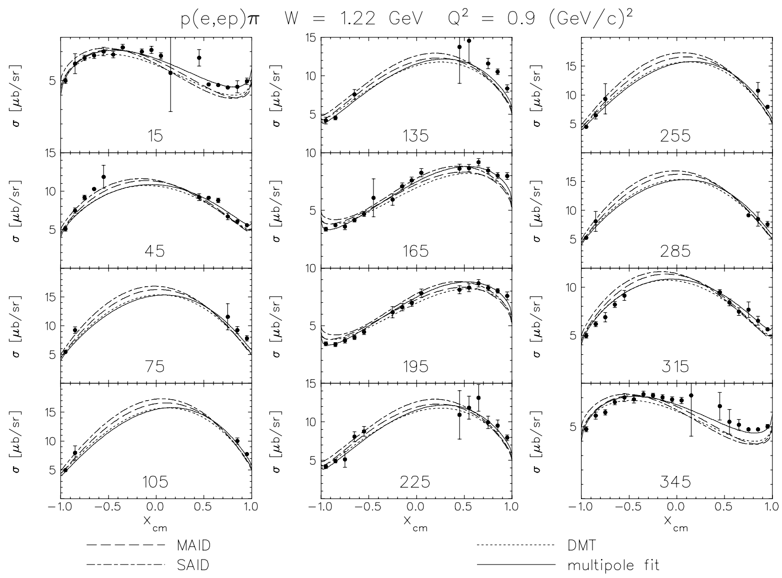

Figure 1: Preliminary cross section data are compared with recent models and a multipole fit. The panels are labeled by ϕ.

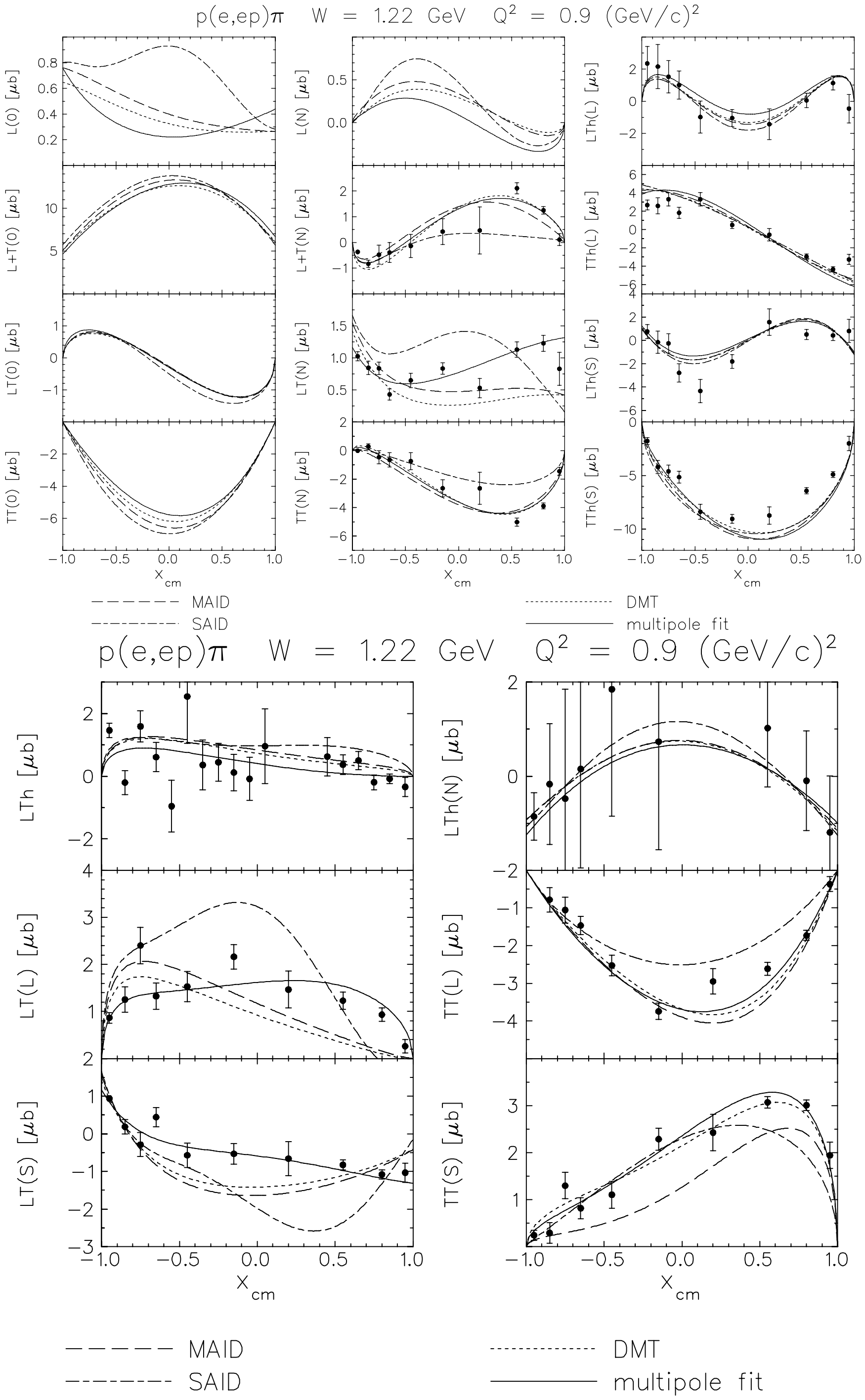

Figure 2: Preliminary data for response functions are compared with recent models and a multipole fit. The top set contribute within the scattering plane while the bottom set requires out-of-plane acceptance. The unpolarized cross sections were included in the multipole fit also but were not decomposed into response functions for this purpose.

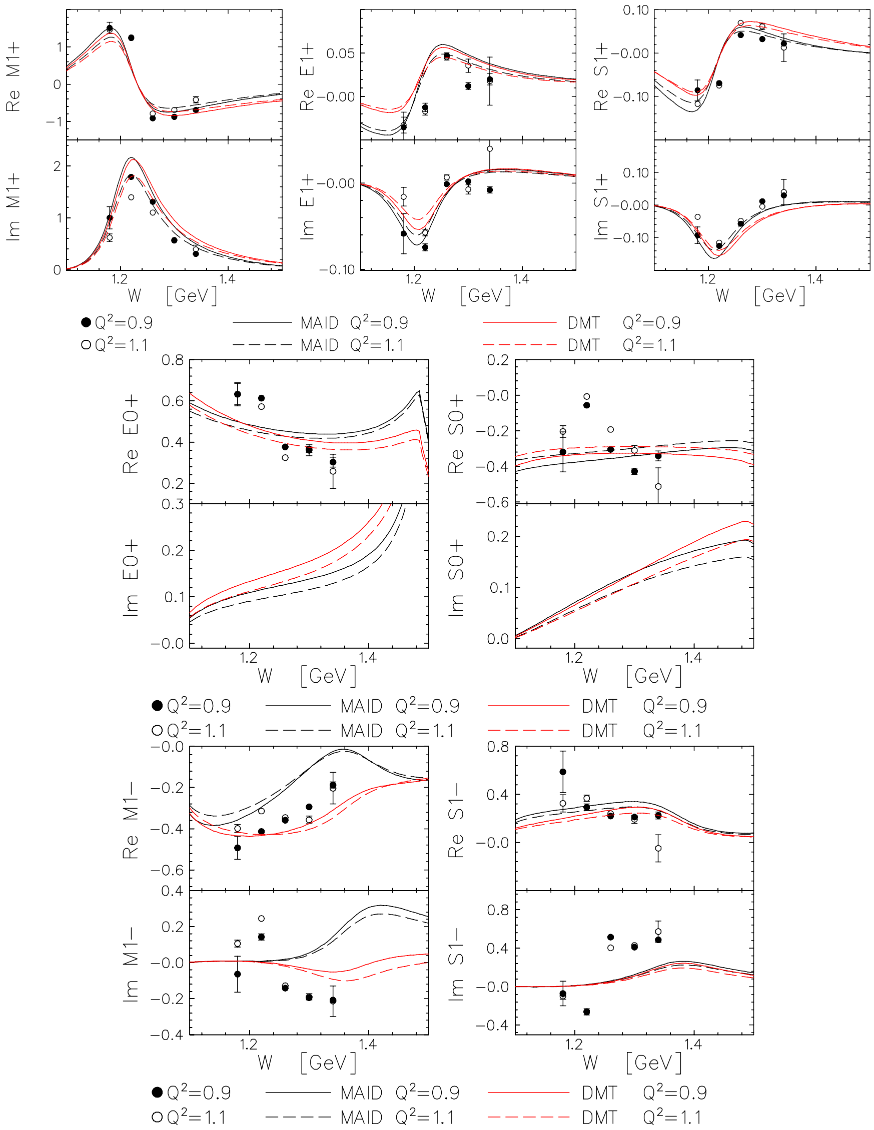

Figure 3: Preliminary 1+ multipole fits. Fitted amplitudes for $Q^2 = 0.9$ or $Q^2 = 1.1$ (GeV$/c)^2$ are shown as filled or open circles, respectively. Baseline (MAID2000) amplitudes for these sets are shown as solid or dashed curves. The corresponding amplitudes for the DMT model are shown in red.